Journal of Orthopaedic Translation 44 (2024) 9–18

Contents lists available at ScienceDirect

Journal of Orthopaedic Translation

journal homepage: www.journals.elsevier.com/journal-of-orthopaedic-translation

Daily low-intensity pulsed ultrasound stimulation mitigates joint degradation and pain in a post-traumatic osteoarthritis rat model

Wonsae Lee [a], Elias Georgas [a], David E. Komatsu [b], Yi-Xian Qin [a,*]

[a] Department of Biomedical Engineering, Stony Brook University, Stony Brook, NY, USA
[b] Department of Orthopaedics and Rehabilitation, Stony Brook University, Stony Brook, NY, USA

ARTICLE INFO

Keywords:
ACLT induced OA
Knee
Knee pain management
LIPUS
Low-intensity pulsed ultrasound
Neuron response
Nociceptive
Osteoarthritis
Osteoclastogenesis

ABSTRACT

Objectives: The aim of this study was to investigate the effects of low-intensity pulsed ultrasound (LIPUS) in a post-traumatic osteoarthritis (OA) rat model and *in vitro*.

Methods: Thirty-eight male, four-month-old Sprague Dawley rats were randomly assigned to Sham, Sham + US, OA, and OA + US. Sham surgery was performed to serve as a negative control, and anterior cruciate ligament transection was used to induce OA. Three days after the surgical procedures, Sham + US and OA + US animals received daily LIPUS treatment, while the rest of the groups received sham ultrasound (US) signals. Behavioral pain tests were performed at baseline and every week thereafter. After 31 days, the tissues were collected, and histological analyses were performed on knees and innervated dorsal root ganglia (DRG) neurons traced by retrograde labeling. Furthermore, to assess the activation of osteoclasts by LIPUS treatment, RAW264.7 cells were differentiated into osteoclasts and treated with LIPUS.

Results: Joint degradation in cartilage and bone microarchitecture were mitigated in OA + US compared to OA. OA + US showed improvements in behavioral pain tests. A significant increase of large soma-sized DRG neurons was located in OA compared to Sham. In addition, a greater percentage of large soma-sized innervated neurons were calcitonin gene-related peptide-positive. Daily LIPUS treatment suppressed osteoclastogenesis *in vitro*, which was confirmed via histological analyses and mRNA expression. Finally, lower expression of netrin-1, a sensory innervation-related protein, was found in the LIPUS treated cells.

Conclusion: Our findings demonstrate that early intervention using LIPUS treatment has protective effects from the progression of knee OA, including reduced tissue degradation, mitigated pain characteristics, improved subchondral bone microarchitecture, and less sensory innervation. Furthermore, daily LIPUS treatment has a suppressive effect on osteoclastogenesis, which may be linked to the suppression of sensory innervation in OA.

The translational potential of this article: This study presents a new potential for early intervention in treating OA symptoms through the use of LIPUS, which involves the suppression of osteoclastogenesis and the alteration of DRG profiles. This intervention aims to delay joint degradation and reduce pain.

1. Introduction

Osteoarthritis (OA) is a chronic degenerative joint disorder associated with debilitating pain. Symptomatic OA is characterized by several hallmarks, including degeneration of cartilage, subchondral bone architectural abnormalities, synovial inflammation, and diverse pain characteristics. Structural dystrophies of the joint tissues are the major microscopic and macroscopic indicators of OA progression. Pain is another critical symptom in symptomatic OA, yet the measure and mechanism of OA pain is very complex, due to the involvement of the nervous system and biochemical factors within the joint [1]. While there are multiple approaches to slowing the progression of OA and mitigating pain, the pathophysiology of OA progression still remains unclear.

Understanding the role of sensory innervation is crucial in mitigating the pain arising from OA. Several previous studies have visualized sensory neurons innervating joints in OA animal models, frequently by using a common sensory neuron marker, calcitonin gene-related peptide (CGRP). The innervating sensory neurons have their cell bodies located in the dorsal root ganglia (DRG). More than 70% of total DRG neurons express CGRP [2,3]. Increased sensory innervation of CGRP-positive neurons has been reported in the monoiodoacetate (MIA) injection and destabilized medial meniscus (DMM) models of OA [2,4–6]. It also has

* Corresponding author. Department of Biomedical Engineering Stony Brook University, 215 Bioengineering Building Stony Brook, NY, 11794, USA.
E-mail address: yi-xian.qin@stonybrook.edu (Y.-X. Qin).

https://doi.org/10.1016/j.jot.2023.09.002
Received 25 May 2023; Received in revised form 22 August 2023; Accepted 12 September 2023

been reported that a larger soma diameter of DRG neurons expressing CGRP innervates the diseased joints in the MIA model of OA [7]. Characterizing nociceptive innervation of nerve fibers in OA is important in understanding OA-related pain, and current literature has begun to elucidate the characteristics and relationships between sensory innervation, OA-related pain, and joint degradation.

Retrograde labeling of innervated sensory neurons allows for the evaluation of afferent neurons. The importance of CGRP-positive neurons has been related to increased osteoclast activity in OA knees [4,8]. Zhu et al. reported that increased osteoclast activity and expression of the protein netrin-1 increases sensory innervation and OA pain using animal models [4]. In the same study, the receptor activator of nuclear factor of kappa-B ligand (RANKL) knockout transgenic mice did not develop OA or OA pain symptoms, indicating osteoclast activity is involved in the symptomatic development. Furthermore, the blockade of netrin-1 in the transgenic mice resulted in attenuated OA symptoms. Therefore, it is suggested that the formation of osteoclasts is associated with OA pathophysiology and further increases sensory innervation to amplify pain signals.

Low-intensity pulsed ultrasound (LIPUS), a non-invasive mechanical stimulus, has shown promising insights in mitigating OA associated pain and cartilage degradation in animal models and clinical settings. It has been shown that suppression of osteoclast activity and bone marrow lesions alleviates OA pain and symptoms [4,8,9]. LIPUS has been reported to induce osteoclast apoptosis and inhibit osteoclastogenesis [10,11]. However, LIPUS has also been reported to enhance osteoclast resorptive activity [12]. With conflicting information in its effect, further investigation into LIPUS stimulation on osteoclasts and further consequences in OA are necessary. Recent publications support the attenuated progression of OA in LIPUS treated animals when the intervention was applied in the relatively early phase of OA pathology [13,14] as well as in mid-late stage OA pathology [15]. Early intervention of LIPUS after anterior cruciate ligament transection (ACLT) induced OA in rats showed higher type II collagen content and lower expression of matrix metalloproteinase-13 (MMP-13) than non-treated ACLT-induced rats [13]. However, the effect of early OA intervention using LIPUS on knee sensory innervation and the involvement of osteoclast suppression in the progression of OA is largely unknown.

Therefore, the primary objective of this study was to investigate the effects of daily LIPUS on degenerating joint symptoms and nociceptive innervation in ACLT model of knee OA. Our secondary objective was to elucidate the effects of LIPUS on osteoclastogenesis. We hypothesized that LIPUS intervention in the early phase of OA would mitigate the progression of the disease with less cartilage degradation, less osteoclast activity, less innervated sensory neurons, and a different profile of CGRP-positive DRG neurons.

2. Methods and materials

2.1. In vivo experimental design

All procedures were reviewed and approved by the Institutional Animal Care and Use Committee at Stony Brook University. Adult four-month-old male Sprague Dawley rats were purchased from Charles River Laboratory. The animals were then randomly assigned to one of the following groups: (1) Sham surgery with Sham LIPUS (Sham, n = 9), (2) Sham surgery with LIPUS (Sham + US, n = 9), (3) OA surgery with Sham LIPUS (OA, n = 10), and (4) OA surgery with LIPUS (OA + US, n = 10). All animals were housed in standard cages with a standard 12 h light/dark cycle. OA surgery groups (OA and OA + US) received anterior cruciate ligament transection (ACLT) surgery on the right knee. The timeline of the experiment is illustrated in Supplementary Fig. 1. All animals were euthanized 31 days post-surgery.

2.2. Daily LIPUS treatment for animals

LIPUS was applied to the medial side of the right knee of the animals using a Sonicator 740 device (Mettler Electronics Corp) with the wave parameters of 3.3 MHz pulse frequency, 0.1 W/cm^2 peak intensity, and 20% duty cycle. The treatment was applied to Sham + US and OA + US groups starting the 4th day after surgery and continuing until the 31st day after surgery. The duration of the treatment was 20min/day, 5 day/week, for 4 weeks. The animals in Sham and OA group were anesthetized for the same duration on the same days that the other groups received treatment with the transducers turned off.

2.3. Behavioral analyses

Pain behavioral tests, including Von Frey filament test, static weight-bearing incapacitance tests, and gait analysis, were performed from baseline to the end of the study once every week, for a total of 5 times throughout the study. A set of Von Frey filaments (Bioseb) was used to measure mechanical allodynia of the animals throughout the course of development of OA and the treatment as described previously [16]. All animals were subjected to the test weekly on an ipsilateral limb. The ascending stimulus method was used on each animal at baseline and every week post-ACLT [17]. The gait of the animals was measured using ink-dipped gait analysis method based on a previously published method. Both hindlimb prints from each animal were analyzed for stride length, step length and toe-out angle based on previous published method [18]. Detailed protocols are described in the supplementary methods.

2.4. Ex-vivo micro computed tomography

To investigate if trabecular epiphyseal trabecular bone is altered by OA pathology and by LIPUS treatment, regions of interest in the subchondral bone of knee samples were scanned by *ex-vivo* X-ray micro-computed tomography (μCT40, Scanco Medical). The knee samples were scanned transversally near the tibial epiphysis using the following parameters; X-Ray peak potential of 55 kVp, an integration time of 200 ms, scanning intensity of 145 μA and a voxel size resolution of 10 μm^3. Circular ROIs were manually drawn to include the medial subchondral trabecular bone and further analyzed using the trabecular bone analysis tools (Gauss sigma:1.2, Gauss support: 2.0, Lower threshold: 362, Higher threshold:1000). Bone morphology parameters including bone volume (BV), bone volume fraction (BV/TV), trabecular number (Tb.N.), thickness (Tb.Th.), and separation (Tb.Sp.), and structural model index (SMI) were analyzed and compared between groups and to the contralateral limb.

2.5. Histological evaluation of knee joint and quantification of osteoclast activity

Half of the preserved joint samples (n = 5) were decalcified in the mix of 8% formic acid and 8% hydrochloric acid for a week with the decalcification solution mix changed daily. The other half of the samples (n = 4–5) were decalcified in 14% EDTA for at least 5 weeks. All decalcified samples were then paraffin embedded and sagittal sections were cut at 8 μm thickness. Safranin O-fast green straining was performed and an OA scoring system was used to determine the grade and stage of OA in each sample [19]. Two distant sections were scored, then the average score was reported for each sample's final score. The samples decalcified using EDTA were stained for tartrate-resistant acid phosphatase 5 b (TRAcP5b or TRAP) activity and osteoclast identification. The protocol was adapted and modified from a previously reported study using open-source histomorphometry software [20]. Three distant sections were histologically assessed for osteoclast surface fraction over bone surface (Oc.S/BS) and

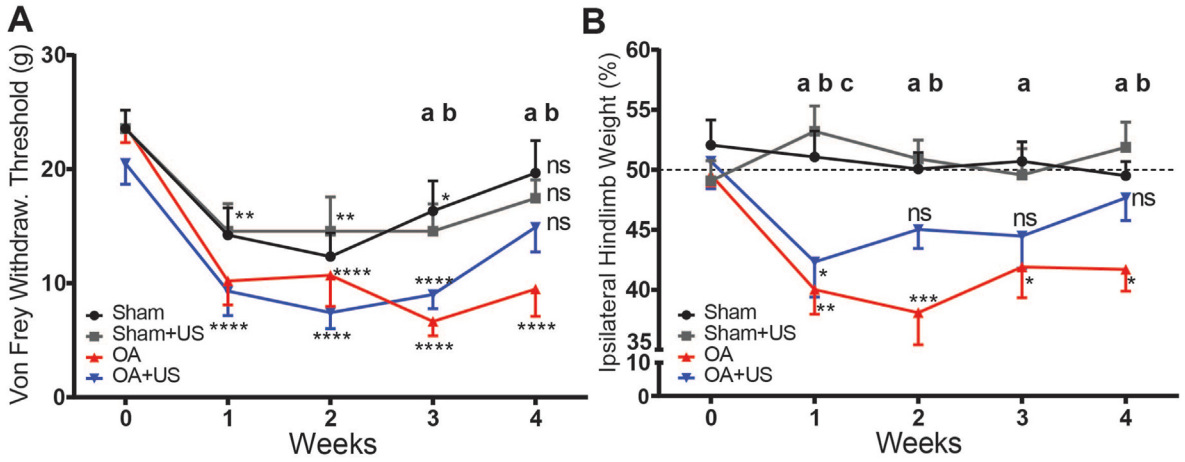

Fig. 1. Ameliorated pain behaviors in the LIPUS treated OA animals in paw withdrawal thresholds and hindlimb weight-bearing **(A)** ACLT induced increased sensitivity in paw withdrawal thresholds but mitigated responses were seen in the LIPUS treated animals in the 4th week (n.s. Sham vs. OA + US, OA + US vs baseline). **(B)** Uneven hindlimb weight-bearing was observed in ACLT animals, but the treated animals did not develop continuous uneven weight-bearing. Statistical differences were calculated with two-way ANOVA; *:$p < 0.05$, **:$p < 0.01$, ***:$p < 0.001$, ****:$p < 0.0001$, a:$p < 0.05$ Sham vs. OA, b:$p < 0.05$ Sham + US vs. OA, c:$p < 0.05$ Sham vs. OA + US. ns: not significant. Results are shown as mean ± SD.

number of osteoclasts per bone surface (N.Oc/BS).

2.6. Immunofluorescence of DRG and knee joint

To visualize the joint innervated neurons, retrograde fluorochrome (Fluoro-Gold, Fluorochrome LLC.) was injected in the intra-articular joint space as previously described [21]. The DRGs were then cryoembedded, sectioned at 20 μm thickness and stored at −20 °C until further immunofluorescence reaction analyses. Immunofluorescence was performed against CGRP-positive and FG-positive neurons (Supplementary Fig. 2A). We first classified all FG-positive neurons and FG- and CGRP-positive neurons based on their soma size. We further stratified the neuronal analyses based on their soma areas to understand the alterations better, based on earlier reported criteria; small ($<600um^2$), medium ($>600um^2$, $<1200um^2$), and large ($>1200um^2$) [7,22]. Then, finally, based on its soma size, the percent distribution of FG-positive neurons, the percent distribution of CGRP-positive neurons per total FG-positive neurons, and the percent alterations of FG- and CGRP-positive neurons under different treatment groups were analyzed. Innervated sensory neurons were visualized and identified under the weight-bearing region using FITC filter.

2.7. In vitro study of cultured osteoclasts and LIPUS treatment

RAW 264.7 cells were seeded in 6-well plates at a density of 80,000 cells. After 24 h, 50 ng/ml of RANKL (R&D Systems, Minneapolis) was added to induce osteoclast differentiation and daily LIPUS treatment began. Cell plates were placed in a degassed water chamber 6 mm above the transducer and were subjected to treatment 20min/day for 7 days (Frequency: 1 MHz, Intensity: 30 mW/cm^2, 20% duty cycle). Control cells underwent same conditions, with the power turned off. Dulbecco's Modified Eagle's Medium (DMEM) supplemented with 10% fetal bovine serum and 1% penicillin-streptomycin was replaced every other day with fresh RANKL until the end of the treatment (n = 3/group). Histological analyses were performed using TRAP staining solution and multinucleated cells were manually counted. Total mRNA was extracted and isolated to determine the osteoclastogenic gene expression levels. Following daily LIPUS treatment, the media of the cultured osteoclasts were collected at day 1, 3, 5 and 7, and ELISAs were performed to determine the amount of netrin-1 and TRAP secretion (Supplementary methods).

2.8. Statistical analysis

All statistics were analyzed using GraphPad Prism software (Version 8.02, GraphPad Software Inc., San Diego). For the *in vivo* study, two-way repeated measure ANOVA with multiple comparisons tests was used to analyze behavioral pain tests. All histological, histomorphometric, immunoreactive analyses, and bone microarchitectural analyses were performed using two-way ANOVA. For the *in vitro* study, histological and qPCR results were compared with Student's t-tests, and ELISA results were compared with two-way ANOVA. All statistically significant differences are noted, where *$p < 0.05$, **$p < 0.01$, ***$p < 0.001$, and ****$p < 0.0001$.

3. Results

3.1. Ameliorated pain behaviors in the LIPUS treated animals

At baseline, the groups did not have a significant difference in mechanical hyperalgesia (Sham 23.5 ± 1.6, Sham + US 23.5 ± 1.6, OA 23.8 ± 1.4, OA + US 20.5 ± 1.8). Both sham and ACLT surgeries caused hyperalgesia by significantly lowering the withdrawal thresholds from their own baseline in the measurements on the 1st and the 2nd weeks post-surgery. On the 3rd week from surgery, the animals in the OA group showed significantly lower withdrawal thresholds compared to sham animals as sham received animals recovered ($p < 0.01$, $p < 0.05$ respectively compared to Sham and Sham + US). The responses from OA + US animals were not significantly different from Sham or Sham + US throughout the study. By the end of the study, OA animals continued to show significantly lowered withdrawal thresholds from their baseline, while all other groups were not significantly different from their baseline measurements (Sham 19.6 ± 2.8, Sham + US 17.4 ± 1.6, OA 9.4 ± 2.3, OA + US 14.9 ± 2.1) (Fig. 1A).

In hindlimb weight-bearing measurements, both Sham and Sham + US animals did not differ from baseline to the end of the study. In the contrast, ACLT animals, both OA and OA + US, showed significantly lowered weight-bearing in their ipsilateral limbs a week after the surgery compared to the baseline (−9%, $p < 0.01$, −8.4%, $p < 0.05$ OA and OA + US respectively). OA + US animals showed ameliorated response from the 2nd week, while OA animals showed continued lowered weight-bearing until the end of the study but not less than 11% from the

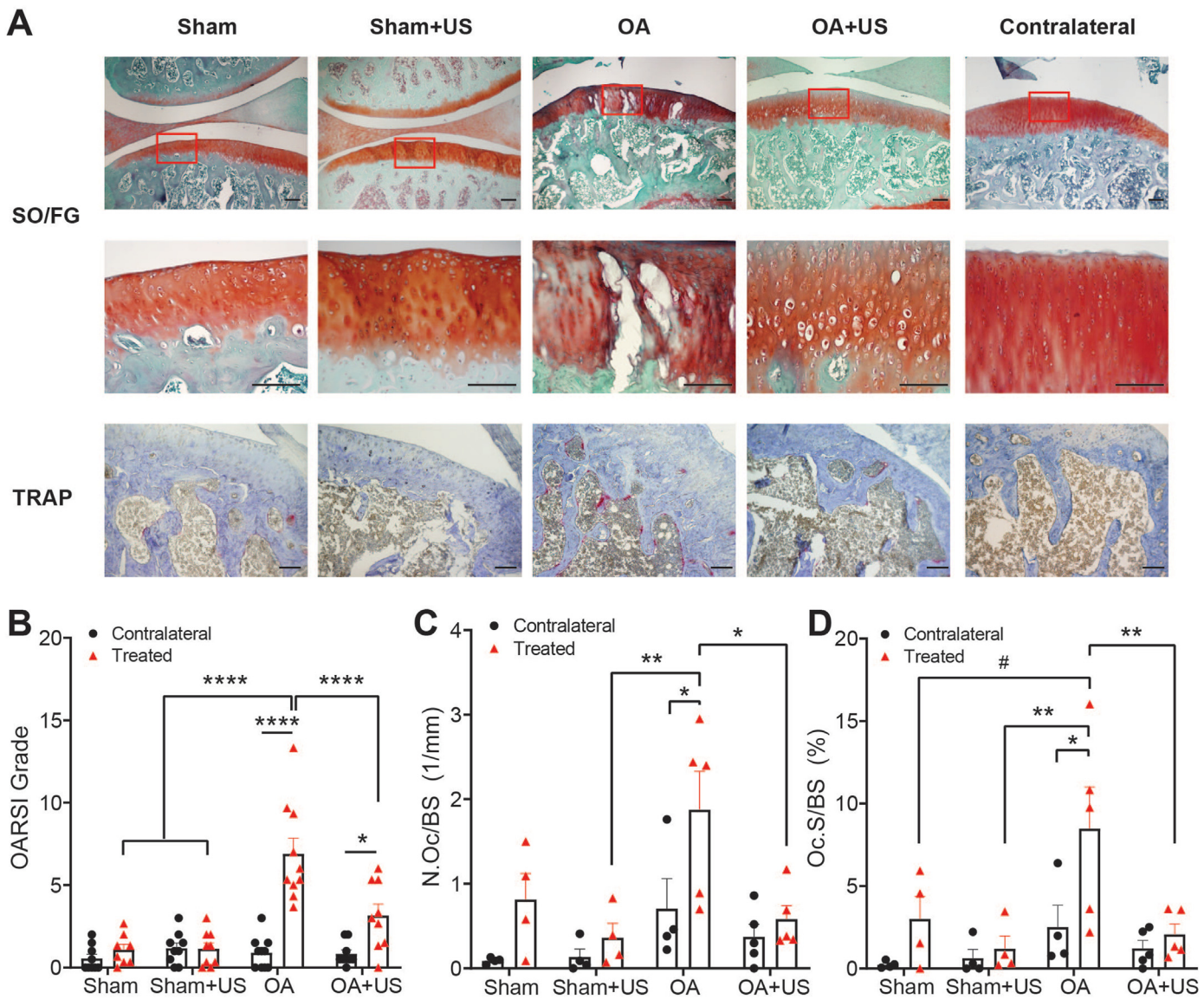

Fig. 2. Histological evaluation of ipsilateral knees **(A)** Safranin O/Fast Green (SO/FG) staining showed degenerated cartilage with lesions in OA animals, while OA + US animals showed less severe developed OA (top row). Magnified image of the red box in the first row (middle row). Increased tartrate-resistant acid phosphate 5 b activity was observed in OA, and suppression of the activity in OA + US (bottom row). Scale bar = 100 μm **(B)** SO/FG scoring showed significantly increased cartilage degeneration in OA and mitigated symptoms in OA + US animals **(C–D)** Osteoclast surface per bone surface (Oc.S/BS) and a number of osteoclasts per bone surface (N.Oc/BS) showed a significant increase in OA animals and reduced expression in OA + US. *:$p < 0.05$, **:$p < 0.01$, ***:$p < 0.001$, ****:$p < 0.0001$, #:$p < 0.10$. Results are shown as mean ± SD. (For interpretation of the references to colour in this figure legend, the reader is referred to the Web version of this article.)

baseline. In the 1st week post-surgery, OA and OA + US animals had significantly lower ipsilateral hindlimb weight-bearing compared the Sham group ($p < 0.01$ and $p < 0.05$, respectively). From the 2nd week to the end of the study, OA + US animals' weight-bearing measurements were not significantly different from Sham animals, while OA animals continued to have significantly lower weight-bearing (Fig. 1B). Unlike mechanical allodynia and reduced weight-bearing in ipsilateral hindlimbs of the animals due to ACLT induced OA, gait analyses did not reveal any significance patterns of the animals based on the surgical procedure or on the LIPUS treatment (Supplementary Fig. 3).

3.2. Cartilage degradation and osteoclast activity were reduced in knee of OA + US animals

The ipsilateral knees of Sham and Sham + US groups showed minimal cartilage degradation after four weeks of treatment and resulted in low OARSI scores. OA group, however, showed lesions in cartilage, enlarged chondrons, and delaminated proteoglycan content in mid zone and deep zone, which resulted in a significantly higher OARSI grade than Sham and Sham + US ($p < 0.0001$). OA + US showed ameliorated histological symptoms after 4 weeks of US treatment (3.16 ± 0.68), significantly different from the OA group ($p < 0.0001$). Compared to their contralateral limbs, both OA and OA + US groups showed significantly higher scores ($p < 0.0001$, $p < 0.05$, respectively) (Fig. 2A and B).

Osteoclast active surface percentage (Oc.S/BS) in the ipsilateral knees of OA group was 5.48%, 7.27%, and 6.41% greater than that of Sham, Sham + US, and OA + US groups ($p = 0.08$, $p < 0.01$, and $p < 0.05$, respectively) (Fig. 2C). The ipsilateral knees of OA group had significantly higher osteoclast active surface percentage than their contralateral knees ($p < 0.05$), while no other animal groups showed any differences compared to their contralateral knees. The number of osteoclasts per bone surface (N.Oc/BS) in the ipsilateral OA group was significantly

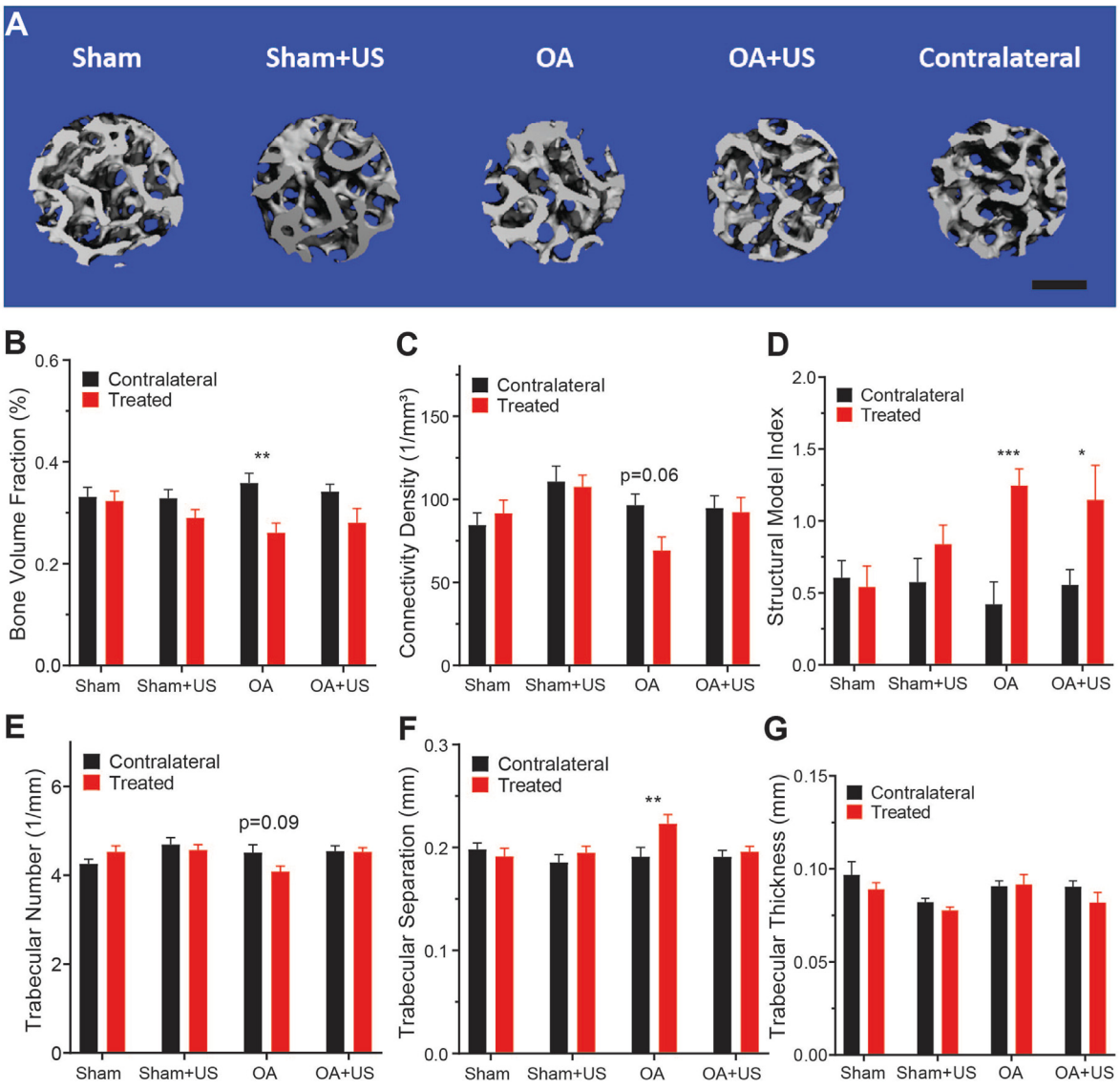

Fig. 3. Micro-computed tomography of subchondral trabecular bone below weight-bearing point **(A)** Representative segmented image of Sham, Sham + US, OA, OA + US and contralateral subchondral bone in cylindrical regions of interest. Scale bar: 500 μm **(B–G)** Microarchitecture analyses of bone volume fraction, connectivity density, structural model index, trabecular number, trabecular thickness and trabecular separation. OA animals showed osteoporotic bone microarchitecture, except in trabecular thickness, compared to its contralateral. OA + US did not have significantly different microarchitecture parameters compared to contralateral except in structural model index. *:$p < 0.05$, **:$p < 0.01$, ***:$p < 0.001$. Results are shown as mean ± SD.

higher than Sham + US and OA + US ($p < 0.01$, $p < 0.05$) (Fig. 2D). Again, only the ipsilateral knees of OA group had a higher number of osteoclasts than their contralateral knees ($p < 0.05$).

3.3. OA showed osteoporotic microarchitecture while OA + US mitigated symptoms

Representative reconstructed images of the weight-bearing subchondral bone in ipsilateral limbs are shown in Fig. 3A. The subchondral bone in knees from the OA group showed significantly lower bone volume fraction, as well as greater structural model index and trabecular separation compared to that of contralateral limbs (Fig. 3B, D, F). Connectivity density and trabecular numbers showed slight but not significant trends of decrease compared to that of contralateral knees ($p = 0.06$, $p = 0.09$ respectively) (Fig. 3C, F). Neither Sham and Sham + US showed a statistical difference in any analyses.

3.4. Increased innervation of large-sized neurons and possible mitigated effect by LIPUS treatment

The soma size of the DRG neurons that were retro-traced was analyzed to determine whether the diseased knees have a higher percentage of sensory innervation and to understand the profiles of the innervations. All somas were analyzed by their size in both FG-positive percentage and FG- and CGRP- positive percentage (Fig. 4A and B). The total number of cells analyzed that were FG-labeled was 1263. After stratifying the size of the neurons into three sub-categories based on their size, Sham animals showed a significantly larger percentage of FG-positive cells (mean percentage, 71%) in small sized neurons than animals from Sham + US, OA, and OA + US (52%, 52%, 57%, respectively) (Fig. 4C). The percentages of large soma DRG neurons present in OA group (12.8%) were significantly higher than that of Sham and Sham + US groups (2.9% and 3.8%), while no significant difference was found in

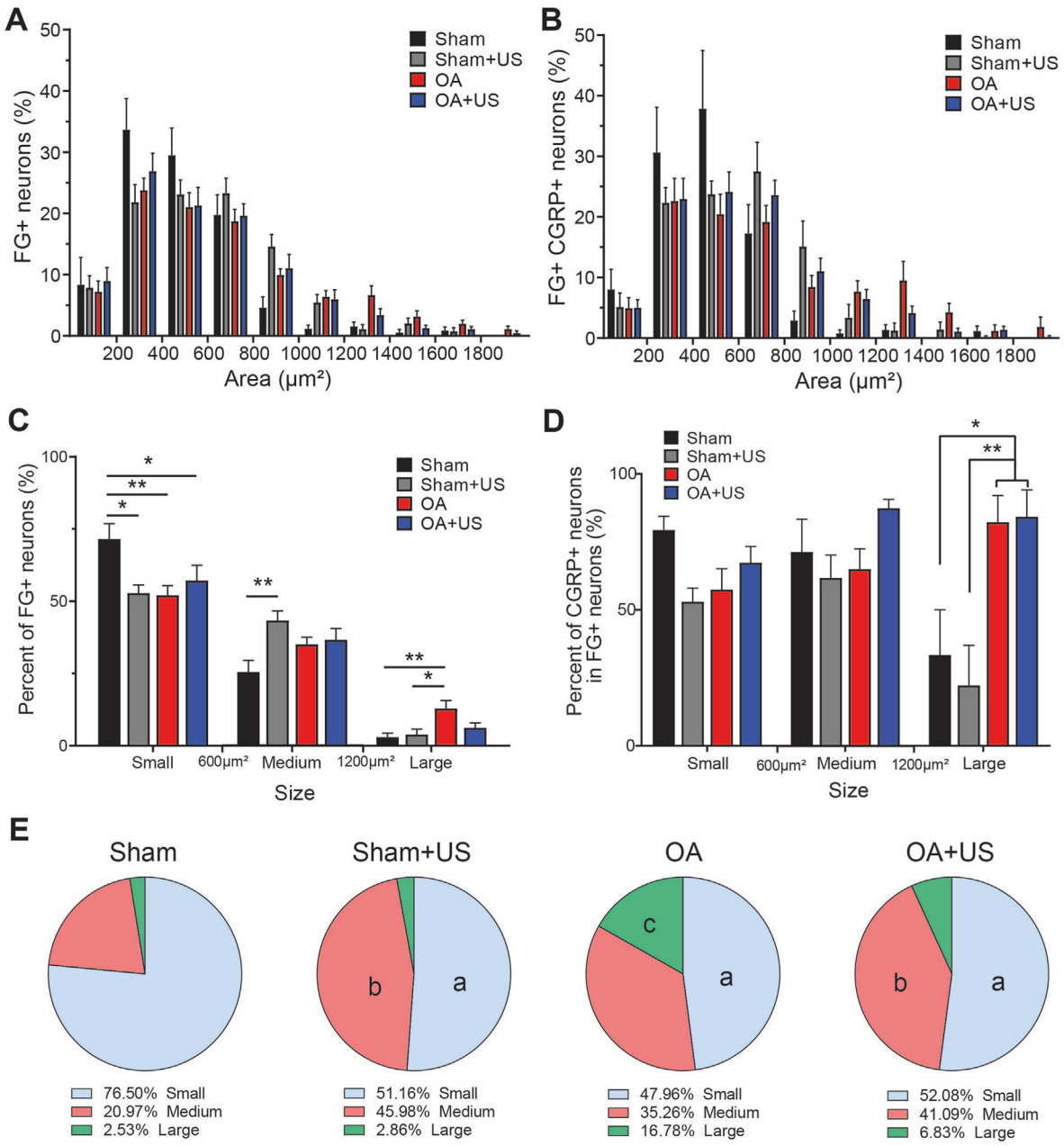

Fig. 4. Increased retrograde-labeled cells in DRG of ACLT induced OA animals in large-sized neurons and slightly reduced by the effect of LIPUS treatment **(A–B)** The percentage of FG-positive and FG-positive CGRP-positive neurons is based on its soma size **(C)** The percentage of FG-positive neurons based on its soma size stratified by subgroups, small (<600 μm^2), medium (>600 μm^2, <1200 μm^2), and large (>1200 μm^2) **(D)** the percentage of CGRP-positive neurons in total FG-positive neurons **(E)** the percentage of FG-positive and CGRP-positive neurons (statistical differences only shown vs. Sham). *:$p < 0.05$, **:$p < 0.01$, a:$p < 0.05$ vs. Sham small, b:$p < 0.05$ vs. Sham medium, c:$p < 0.05$ vs. Sham large. Results are shown as mean ± SD.

OA + US group (6.2%). A similar trend was also found in the total number of FG-positive neurons (Supplementary Fig. 3B).

The percentage of CGRP-positive neurons in total FG-positive cells was then analyzed to understand whether there is a peptidergic shift in DRG neurons (Fig. 4D). In the small- and medium-sized neurons, there was not a statistical difference between groups. However, in large-sized neurons, more than 80% of FG-positive cells in OA and OA + US were CGRP-positive, while less than 40% of FG-positive cells were CGRP-positive in Sham and Sham + US ($p < 0.05$).

Then the percentage of CGRP-positive and FG-positive was calculated to understand the profile (Fig. 4E). Sham had a significantly higher percentage of small-size compared to the rest of the groups (76.5% vs. 51.16%, 47.96%, and 52.08%, $p < 0.05$). OA group showed a significant increase in large-size neurons (Sham 2.53% vs. OA 16.78%, $p < 0.05$). However, OA + US group did not show a statistical difference in the percentage of large-size CGRP-positive and FG-positive neurons when compared to Sham, Sham + US, and OA groups. Finally, sensory innervation was visualized in the subchondral bone marrow of ipsilateral knee (Fig. 5). While CGRP-positive sensory neurons were easily visualized in the knees of OA animals, they were not present in the knees of Sham, Sham + US, and OA + US animals.

3.5. *LIPUS suppresses osteoclastogenesis in vitro*

Histological evaluation revealed that daily LIPUS treatment significantly suppressed the formation of TRAP positive multi-nucleated osteoclasts ($p < 0.01$, Fig. 6A and B). Furthermore, LIPUS significantly reduced osteoclast-specific expression of *NFATc-1*, *cathepsin-K*, and *TRAP*

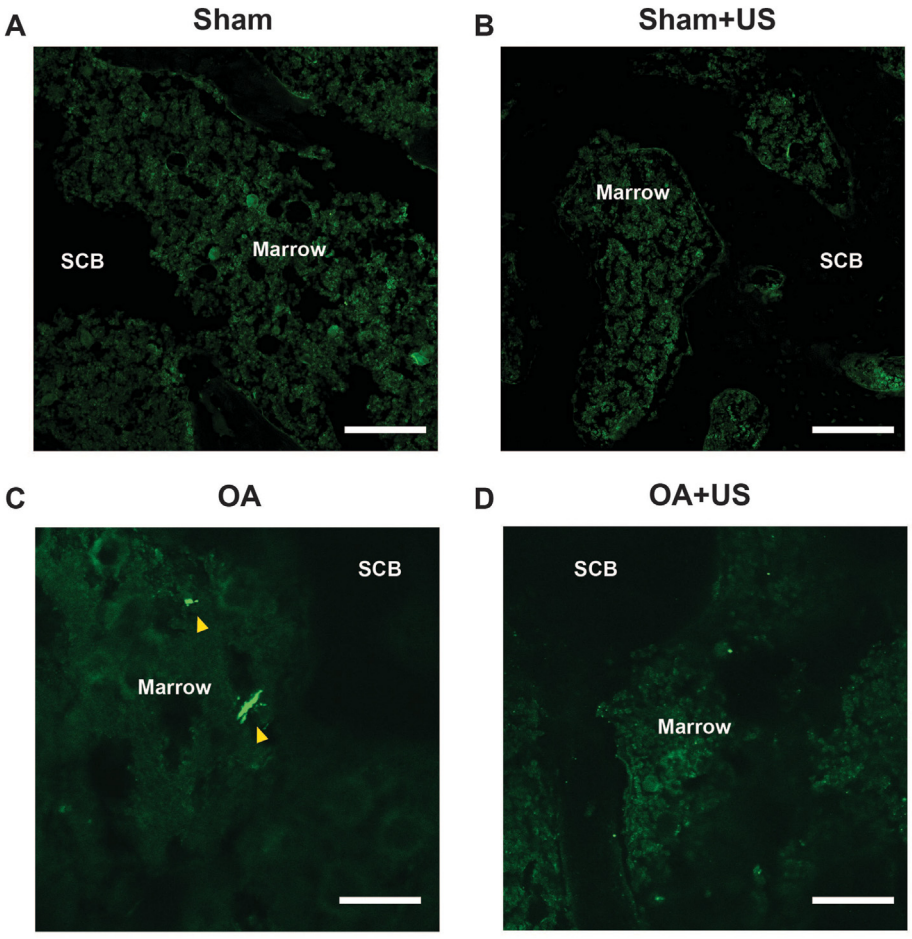

Fig. 5. Representative images of immunofluorescence for calcitonin gene-related peptide-positive (CGRP-positive) in subchondral bone marrow Immunofluorescence staining of CGRP-positive fibers in **(A)** Sham **(B)** Sham + US **(C)** OA, and **(D)** OA + US. OA animals showed increased CGRP-positive fibers (arrowhead) in subchondral bone marrow space. Scale bar: 100 μm.

($p < 0.05$), while there were no significant differences in *osteopontin* and *COX-2* (Fig. 6C). In addition, protein analysis via ELISA showed significant reduction of TRAP secretion after day 5 that continued to day 7 of LIPUS treatment ($p < 0.01$ and $p < 0.001$, respectively, Fig. 6D). Interestingly, LIPUS significantly reduced the mRNA expression of the axonal guidance protein and *netrin-1* ($p < 0.05$, Fig. 6C). To further investigate the role of netrin-1 in osteoclast activity, secretion of netrin-1 was monitored via ELISA. There was a significant secretion reduction by day 5 which was further reduced by day 7 ($p < 0.05$, Fig. 6E).

4. Discussion

OAis a degenerative disease with multifactorial symptoms and debilitating pain. Suppression of OA symptoms is limited due to the involvement of many tissue types and their heterogeneity. This study evaluated the potential of using daily LIPUS treatment as a preventative modality for the symptoms of OA induced by ACLT in a rat model. ACLT created a symptomatic OA animal model in four weeks, with histological degradation of cartilage, high percentage of osteoclast activity, osteoporotic subchondral bone microarchitecture, pain-related behaviors, and higher sensory innervation. With early intervention using LIPUS, the symptoms of OA were maintained or reversed to prevent the development of OA. In addition, our results suggest that LIPUS treatment suppresses osteoclastogenesis and secretion of netrin-1, which may help explain the pain mitigation seen *in vivo*. To our best knowledge, this is the first study to evaluate the effect of LIPUS on phenotypic alterations of knee innervating DRG neurons. Moreover, this is the first study to investigate the effect of LIPUS on osteoclast suppression in a rat animal OA model as well as *in vitro*.

In the current study, ACLT animals showed osteoarthritic symptoms, including hyperalgesia and uneven weight loading behaviors, decreased cartilage integrity, osteoporotic subchondral bone, and increased sensory innervation within four weeks of the surgical procedure. Barbosa and colleagues reported similar results that ACLT induces signs of OA in rats regarding its pain, functional impairment, and synovial inflammation in thirty days compared to longer developed OA [23]. Mechanical allodynia and weight-bearing of ipsilateral hindlimbs were significantly affected by ACLT in two weeks. However, the LIPUS treated OA-induced animals showed blunted pain responses by the fourth week. This reveals the capability of LIPUS in preventing and mitigating OA-related pain behavioral symptoms. Although there was successful mitigation of pain symptoms, gait analysis revealed no correlation to the development of pain. One possible explanation could be that the measures of gait in the ink-dipped method are limited in terms of missing temporal elements. A more precise method such as digitalized Cat-Walk analysis may be needed to test the further development of OA symptoms.

Numerous studies have described the possible involvement of CGRP-positive innervated neurons in developing weight-bearing pain. Although many studies of CGRP and OA pain used MIA animal models, a few studies highlighted the similar occurrence of CGRP-positive innervation in OA knee and altered nociceptive characteristic in joint instability animal models [4,24,25]. The increased number of nociceptive neurons in subchondral bone was also found to be localized in osteochondral channels, which are vascular channel breaks in the tidemark

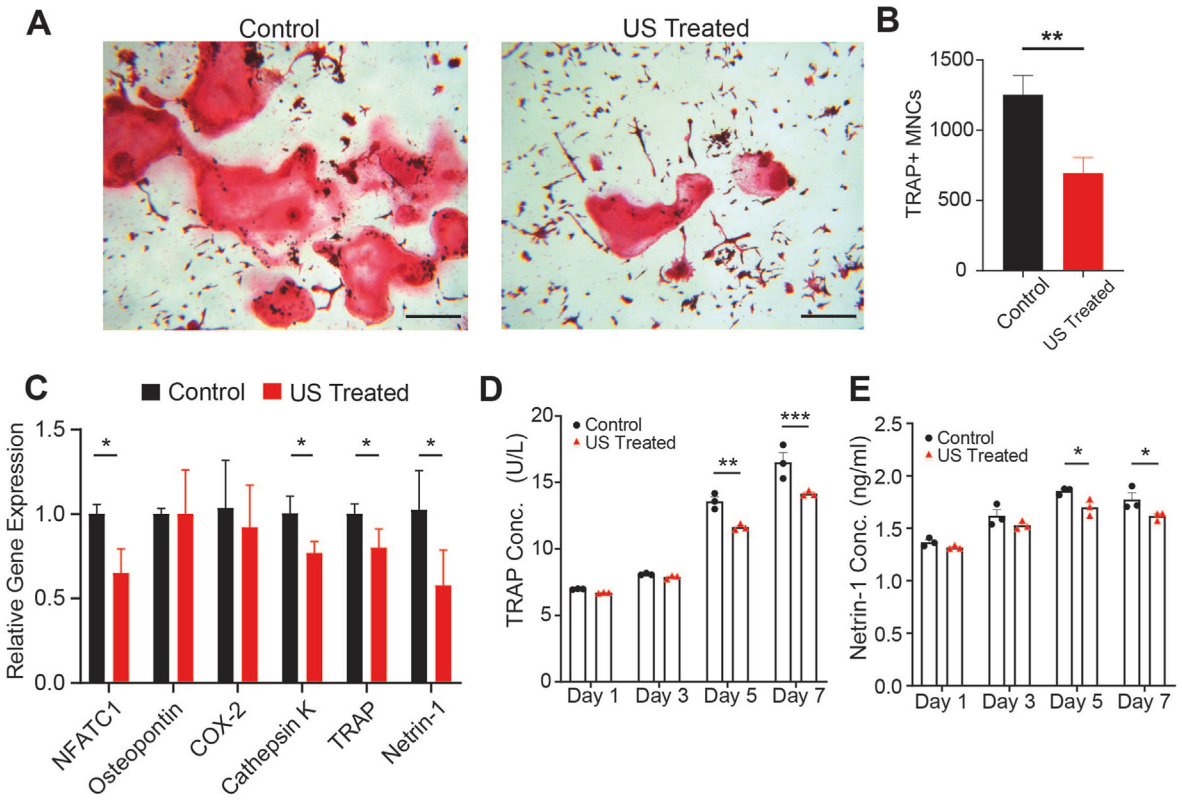

Fig. 6. LIPUS suppresses osteoclastogenesis and netrin-1 secretion **(A)** Representative images of TRAP-stained osteoclasts, scale bar: 200 μm **(B)** Quantification of TRAP-positive multinucleated cells shows inhibition of osteoclast formation following 7 days of LIPUS treatment **(C)** LIPUS significantly inhibits osteoclastogenic gene expression levels **(D–E)** LIPUS reduces TRAP and netrin-1 secretion measured in cell media over time measured via ELISA. *:$p < 0.05$, **:$p < 0.01$, ***:$p < 0.001$, TRAP: Tartrate-resistant acid phosphatase, Results are shown as mean ± SD.

between subchondral bone and the deep layer of cartilage below the weight-bearing point [24,26]. The innervation of large CGRP-positive retrograde labeled DRGs in OA knee was reported in the MIA model of OA [2,7]. The high percentage of DRG neurons of large soma size may also indicate a different pain sensitization profile compared to newly introduced pain in OA. The difference in the soma size might be coupled to a different sensitization profile to the introduced chronic pain, and further affected pain behaviors, as reported in earlier report [27]. A significantly lower percentage of CGRP-positive large size neurons in Sham animals contrasts with a higher percentage of CGRP-positive in the innervated neurons in OA animals (Fig. 4G). OA animals treated with LIPUS treatment showed a 59.3% decrease in CGRP-positive FG-positive neurons, possibly explaining the mitigated pain sensation.

The correlation of the expression of osteoclasts and OA pathology with pain symptoms was discussed in several studies in preclinical studies [4,28] and a clinical study [29]. A similar trend was observed in our study as well, in which ACLT-received animals had a higher osteoclast activity with high pain symptoms compared to both the contralateral and sham controls (Fig. 2). Interestingly, LIPUS treatment suppressed osteoclast activity and osteoclastogenesis significantly *in vivo* and *in vitro*. It has been reported that LIPUS stimulation increases prostaglandin E_2 (PGE_2) secretion from osteoblasts, which inhibits osteoclast formation [30]. More recently, a mechanosensitive calcium-activated chloride channel, anoctamin-1 (Ano1), was downregulated in response to mechanical stimulation in osteoclasts and inhibited their activity [31]. Taken together, it is likely that LIPUS may directly and indirectly inhibit osteoclasts through Ano1 and osteoblast PGE_2 production, respectively, that will be evaluated in future studies. In addition, there is great interest in whether the beneficial treatment effect of LIPUS in cartilage tissue was triggered upon focal adhesion kinase and kindlin-2 as the key cartilage integrity proteins [32,33]. The micro-CT analyses conveyed the result of the suppression of the catabolic activity, indicating that LIPUS acted as a preventative measure of high bone resorption in OA possibly suppressing the formation of bone marrow lesions. The suppression of the catabolic activity in OA by bisphosphonates was successful in reducing pain behavior in an OA animal model [8] and a clinical study [34] as well. In addition, the catabolic activity measured by serum TRAcP5b level was positively correlated with knee OA pain in a clinical setting [35]. As the study delineated, the suppression of the osteoclast activity by the LIPUS treatment is essential information for the pain mitigating mechanism in early OA. Expanding the depth of analyses to other biomarkers of bone resorption, i.e., RANKL/OPG ratio and circulating cathepsin K, is needed to eliminate the possibility that the increased TRAcP5b activity is from macrophages or other dendritic cells *in vivo*. Interestingly, LIPUS did not result in a higher bone mass or suppression of osteoclast activity in Sham + US animals, showing a possible interaction of the diseased state and the effect of LIPUS may exist. Similarly, LIPUS brought a higher anabolic potential in osteoporotic bone than healthy in fracture healing [36] and in retaining bone microarchitecture in disuse animal model [37]. Thus, the mechanism of LIPUS may act better against the abnormal condition of high catabolic activity.

LIPUS has been widely applied for bone fracture healing and non-unions as a non-invasive mechanical stimulus. However, its coupling effect with CGRP has been reported in a spinal fusion study where LIPUS promoted CGRP-mediated spinal fusion and ectopic bone formation [38]. This contradictory effect of LIPUS from the current study may arise from different transmitting frequencies of the ultrasound (3 MHz vs. 1.5 MHz). Currently, it is challenging to predict CGRP expressing sensory innervation responses to mechanical stimulus, especially when the neurons are surrounded by bone tissue, which will enhance the anabolic pathway. In a study from Lam and colleagues, accelerated fracture repair by LIPUS was inhibited in rats with neural injury [39]. This may indicate a

differential effect of LIPUS on bone depending on the intactness of its innervation. Our understanding of the different responses in CGRP-positive neurons is still limited and future studies need to elucidate the contradictory effect of LIPUS. Analyzing pain mechanisms with molecular pathways such as the nerve growth factor – tropomyosin receptor kinase A (NGF-TrkA) signaling pathway, one of the mediators of OA pain signaling [25,40,41], could be targeted to understand how LIPUS directly or indirectly affects sensory innervation. Our results suggest that communication between osteoclasts and sensory neurons may be a possible mechanism of LIPUS innervation mitigation in OA. Netrin-1 secretion by increased activity of osteoclasts in subchondral bone resorption induced sensory innervation and OA pain, while knockout of netrin-1 in osteoclasts reduced OA pain behavior [4]. In this study, we showed that LIPUS mitigated the activity and formation of osteoclasts, resulting in reduced netrin-1 secretion and sensory innervation. This reduction in netrin-1 secretion may give some mechanistic insight into the reduced OA innervation under LIPUS treatment seen *in vivo*. However, a more detailed analysis of the molecular signaling pathway involvement is necessary to gain new insights into the primary and secondary mechanotransductive effects of CGRP-positive innervation upon LIPUS treatment.

There are several limitations to the current study. First, the retrograde labeling only traced neurons in the intra-articular space of knee joints, and was not targeted to the subchondral bone, where sensory innervation was visualized and analyzed. Thus, the retrograde labels might have been traced to other innervated tissues, such as synovium. However, a strong inflammatory response might arise when injecting retrograde labels into subchondral bone since it involves drilling a hole [7]. Therefore, this spike in inflammation may be a problem, especially within a relatively short duration of the experiment. Second, the study did not examine the mechanism by which LIPUS suppresses osteoclast activity and inhibits sensory innervation. Further studies with transgenic animal models would be necessary for a deeper understanding of these mechanisms. Third, the study did not analyze the direct effects of LIPUS on neurons through mechanosensitive channels such as voltage-gated sodium channel (Na_V) and transient receptor potential cation channels (TRPs) [42,43]. Though this study is to comprehend the alterations of innervation in OA and with respect to the interaction between bone cells, the direct effects should not be neglected.

In summary, the present study collectively shows that LIPUS has mitigative characteristics in early symptomatic OA development and pain related sensory innervation in a rat model of post-traumatic OA. Therefore, these findings may contribute to a better understanding of the use of LIPUS in early symptomatic OA treatment in the clinical setting.

ICMJE COI statement

None of the authors have any conflicts of interest associated with this study.

Funding statement

The authors disclose receipt of the following financial or material support for the research, authorship, and/or publication of this article: Scholars in Biomedical Sciences Program (T32GM127253). The study is supported by NIH (R01AR061821, YXQ), and partially by NSF (ECCS 2020867, YXQ).

Declaration of competing interest

The authors declare that they have no known competing financial interests or personal relationships that could have appeared to influence the work reported in this paper.

Acknowledgments

The authors are grateful to Dr. Clinton Rubin for valuable insight and discussions. The authors would also like to acknowledge Kaitlyn Chua, and the members at the Orthopaedic Bioengineering Lab for helping with the maintenance associated with the study and technical support. Graphical abstract was created with Biorender.com.

Appendix A. Supplementary data

Supplementary data to this article can be found online at https://doi.org/10.1016/j.jot.2023.09.002.

References

[1] Chen D, Shen J, Zhao W, Wang T, Han L, Hamilton JL, et al. Osteoarthritis: toward a comprehensive understanding of pathological mechanism. Bone Res 2017. https://doi.org/10.1038/boneres.2016.44.
[2] Ferreira-Gomes J, Adães S, Sarkander J, Castro-Lopes JM. Phenotypic alterations of neurons that innervate osteoarthritic joints in rats. Arthritis Care Res 2010;62:3677–85. https://doi.org/10.1002/art.27713.
[3] Staton PC, Wilson AW, Bountra C, Chessell IP, Day NC. Changes in dorsal root ganglion CGRP expression in a chronic inflammatory model of the rat knee joint: differential modulation by rofecoxib and paracetamol. Eur J Pain 2007. https://doi.org/10.1016/j.ejpain.2006.03.006.
[4] Zhu S, Zhu J, Zhen G, Hu Y, An S, Li Y, et al. Subchondral bone osteoclasts induce sensory innervation and osteoarthritis pain 2019;129:1076–93. https://doi.org/10.1172/JCI121561.
[5] Walsh DA, Mapp PI, Kelly S. Calcitonin gene-related peptide in the joint: contributions to pain and inflammation. Br J Clin Pharmacol 2015;80:965–78. https://doi.org/10.1111/bcp.12669.
[6] Grässel S, Muschter D. Peripheral nerve fibers and their neurotransmitters in osteoarthritis pathology. Int J Mol Sci 2017;18. https://doi.org/10.3390/ijms18050931.
[7] Aso K, Izumi M, Sugimura N, Okanoue Y, Ushida T, Ikeuchi M, et al. Nociceptive phenotype alterations of dorsal root ganglia neurons innervating the subchondral bone in osteoarthritic rat knee joints. Osteoarthritis Cartilage 2016;24:1596–603. https://doi.org/10.1016/j.joca.2016.04.009.
[8] Yu D, Liu F, Liu M, Zhao X, Wang X, Li Y, et al. The inhibition of subchondral bone lesions significantly reversed the weight-bearing deficit and the overexpression of CGRP in DRG neurons, GFAP and Iba-1 in the spinal dorsal horn in the monosodium iodoacetate induced model of osteoarthritis pain. PLoS One 2013. https://doi.org/10.1371/journal.pone.0077824.
[9] Alliston T, Hernandez CJ, Findlay DM, Felson DT, Kennedy OD. Bone marrow lesions in osteoarthritis: what lies beneath. J Orthop Res 2018. https://doi.org/10.1002/jor.23844.
[10] Carina V, Costa V, Pagani S, De Luca A, Raimondi L, Bellavia D, et al. Inhibitory effects of low intensity pulsed ultrasound on osteoclastogenesis induced in vitro by breast cancer cells. J Exp Clin Cancer Res 2018. https://doi.org/10.1186/s13046-018-0868-2.
[11] Meng J., Hong J., Zhao C., Zhou C., Hu B., Yang Y., et al. Low-intensity pulsed ultrasound inhibits rankl-induced osteoclast formation via modulating ERK-c-Fos-NFATc1 signaling cascades. Am J Transl Res 2018. Sep 15;10(9):2901-2910.
[12] Feres MFN, Kucharski C, Diar-Bakirly S, El-Bialy T. Effect of low-intensity pulsed ultrasound on the activity of osteoclasts: an in vitro study. Arch Oral Biol 2016;70:73–8. https://doi.org/10.1016/j.archoralbio.2016.06.007.
[13] Hsieh YL, Chen HY, Yang CC. Early intervention with therapeutic low-intensity pulsed ultrasound in halting the progression of post-traumatic osteoarthritis in a rat model. Ultrasound Med Biol 2018. https://doi.org/10.1016/j.ultrasmedbio.2018.08.007.
[14] Naito K, Watari T, Muta T, Furuhata A, Iwase H, Igarashi M, et al. Low-intensity pulsed ultrasound (LIPUS) increases the articular cartilage type II collagen in a rat osteoarthritis model. J Orthop Res 2010;28:361–9. https://doi.org/10.1002/jor.20995.
[15] Li X, Sun Y, Zhou Z, Zhang D, Jiao J, Hu M, et al. Mitigation of articular cartilage degeneration and subchondral bone sclerosis in osteoarthritis progression using low-intensity ultrasound stimulation. Ultrasound Med Biol 2019;45:148–59. https://doi.org/10.1016/j.ultrasmedbio.2018.08.022.
[16] Tsai H-C, Chen T-L, Chen Y-P, Chen R-M. Traumatic osteoarthritis-induced persistent mechanical hyperalgesia in a rat model of anterior cruciate ligament transection plus a medial meniscectomy. J Pain Res 2017;11:41–50. https://doi.org/10.2147/JPR.S154038.
[17] Deuis JR, Dvorakova LS, Vetter I. Methods used to evaluate pain behaviors in rodents. Front Mol Neurosci 2017;10:1–17. https://doi.org/10.3389/fnmol.2017.00284.
[18] Jacobs BY, Kloefkorn HE, Allen KD. Gait analysis methods for rodent models of osteoarthritis. Curr Pain Headache Rep 2014;18:456. https://doi.org/10.1007/s11916-014-0456-x.

[19] Pritzker Kphkph, Gay S, Jimenez SAA, Ostergaard K, Pelletier J-PP, Revell K, et al. Osteoarthritis cartilage histopathology: grading and staging. Osteoarthritis Cartilage 2006;14:13–29. https://doi.org/10.1016/j.joca.2005.07.014.
[20] van 't Hof RJ, Rose L, Bassonga E, Daroszewska A. Open source software for semi-automated histomorphometry of bone resorption and formation parameters. Bone 2017;99:69–79. https://doi.org/10.1016/j.bone.2017.03.051.
[21] Yu D, Yu B, Mao Y, Zhao X, Wang X, Ding H, et al. Efficacy of zoledronic acid in treatment of teoarthritis is dependent on the disease progression stage in rat medial meniscal tear model. Acta Pharmacol Sin 2012;33:924–34. https://doi.org/10.1038/aps.2012.28.
[22] Franken G, Douven P, Debets J, Joosten EAJ. Conventional dorsal root ganglion stimulation in an experimental model of painful diabetic peripheral neuropathy: a quantitative immunocytochemical analysis of intracellular γ-aminobutyric acid in dorsal root ganglion neurons. Neuromodulation 2021;24:639–45. https://doi.org/10.1111/ner.13398.
[23] Barbosa GM, Cunha JE, Russo TL, Cunha TM, Castro PATS, Oliveira FFB, et al. Thirty days after anterior cruciate ligament transection is sufficient to induce signs of knee osteoarthritis in rats: pain, functional impairment, and synovial inflammation. Inflamm Res 2020;69:279–88. https://doi.org/10.1007/s00011-020-01317-1.
[24] Aso K, Shahtaheri SM, Hill YZR, Wilson YZD, Mcwilliams DF, Nwosu LN, et al. Contribution of nerves within osteochondral channels to osteoarthritis knee pain in humans and rats. 2020. https://doi.org/10.1016/j.joca.2020.05.010.
[25] Nwosu LN, Mapp PI, Chapman V, Walsh DA. Blocking the tropomyosin receptor kinase A (TrkA) receptor inhibits pain behaviour in two rat models of osteoarthritis. Ann Rheum Dis 2016. https://doi.org/10.1136/annrheumdis-2014-207203.
[26] Eitner A, Hofmann GO, Schaible H-G. Mechanisms of osteoarthritic pain. Studies in humans and experimental models. Front Mol Neurosci 2017;10:1–22. https://doi.org/10.3389/fnmol.2017.00349.
[27] Aso K, Ikeuchi M, Izumi M, Sugimura N, Kato T, Ushida T, et al. Nociceptive phenotype of dorsal root ganglia neurons innervating the subchondral bone in rat knee joints. Eur J Pain 2014. https://doi.org/10.1002/j.1532-2149.2013.00360.x.
[28] Zhen G, Cao X. Targeting TGFβ signaling in subchondral bone and articular cartilage homeostasis. Trends Pharmacol Sci 2014. https://doi.org/10.1016/j.tips.2014.03.005.
[29] Zhou F, Han X, Wang L, Zhang W, Cui J, He Z, et al. Associations of osteoclastogenesis and nerve growth in subchondral bone marrow lesions with clinical symptoms in knee osteoarthritis. J Orthop Transl 2022;32:69–76. https://doi.org/10.1016/j.jot.2021.11.002.
[30] Sun JS, Hong RC, Chang WHS, Chen LT, Lin FH, Liu HC. In vitro effects of low-intensity ultrasound stimulation on the bone cells. J Biomed Mater Res 2001;57:449–56. https://doi.org/10.1002/1097-4636(20011205)57:3<449::AID-JBM1188>3.0.CO;2-0.
[31] Sun W, Li Y, Li J, Tan Y, Yuan X, Meng H, et al. Mechanical stimulation controls osteoclast function through the regulation of Ca2+-activated Cl− channel Anoctamin 1. Commun Biol 2023;6. https://doi.org/10.1038/s42003-023-04806-1.
[32] Chen S, He T, Zhong Y, Chen M, Yao Q, Chen D, et al. Roles of focal adhesion proteins in skeleton and diseases. Acta Pharm Sin B 2023;13:998–1013. https://doi.org/10.1016/j.apsb.2022.09.020.
[33] Wu X, Lai Y, Chen S, Zhou C, Tao C, Fu X, et al. Kindlin-2 preserves integrity of the articular cartilage to protect against osteoarthritis. Nat Aging 2022;2:332–47. https://doi.org/10.1038/s43587-021-00165-w.
[34] Laslett LL, Doré DA, Quinn SJ, Boon P, Ryan E, Winzenberg TM, et al. Zoledronic acid reduces knee pain and bone marrow lesions over 1 year: a randomised controlled trial. Ann Rheum Dis 2012;71:1322–8. https://doi.org/10.1136/annrheumdis-2011-200970.
[35] Nwosu LN, Allen M, Wyatt L, Huebner JL, Chapman V, Walsh DA, et al. Pain prediction by serum biomarkers of bone turnover in people with knee osteoarthritis: an observational study of TRAcP5b and cathepsin K in OA. Osteoarthritis Cartilage 2017;25:858–65. https://doi.org/10.1016/j.joca.2017.01.002.
[36] Cheung WH, Chin WC, Qin L, Leung KS. Low intensity pulsed ultrasound enhances fracture healing in both ovariectomy-induced osteoporotic and age-matched normal bones. J Orthop Res 2012. https://doi.org/10.1002/jor.21487.
[37] Uddin SMZ, Qin YX. Dynamic acoustic radiation force retains bone structural and mechanical integrity in a functional disuse osteopenia model. Bone 2015. https://doi.org/10.1016/j.bone.2015.01.020.
[38] Zhou X-YY, Xu X-MM, Wu S-YY, Wang F, Zhang Z-CC, Yang Y-LL, et al. Low-intensity pulsed ultrasound-induced spinal fusion is coupled with enhanced calcitonin gene-related peptide expression in rat model. Ultrasound Med Biol 2017;43:1486–93. https://doi.org/10.1016/j.ultrasmedbio.2017.03.012.
[39] Lam WL, Guo X, Leung KS, Kwong KSC. The role of the sensory nerve response in ultrasound accelerated fracture repair. J Bone Jt Surg - Ser B 2012. https://doi.org/10.1302/0301-620X.94B10.29139.
[40] Nencini S, Ringuet M, Kim DH, Chen YJ, Greenhill C, Ivanusic JJ. Mechanisms of nerve growth factor signaling in bone nociceptors and in an animal model of inflammatory bone pain. Mol Pain 2017. https://doi.org/10.1177/1744806917697011.
[41] Mantyh PW, Koltzenburg M, Mendell LM, Tive L, Shelton DL. Antagonism of nerve growth factor-TrkA signaling and the relief of pain. Anesthesiology 2011. https://doi.org/10.1097/ALN.0b013e31821b1ac5.
[42] Burks SR, Lorsung RM, Nagle ME, Tu T-W, Frank JA. Focused ultrasound activates voltage-gated calcium channels through depolarizing TRPC1 sodium currents in kidney and skeletal muscle. Theranostics 2019;9:5517–31. https://doi.org/10.7150/thno.33876.
[43] Tyler WJ, Tufail Y, Finsterwald M, Tauchmann ML, Olson EJ, Majestic C. Remote excitation of neuronal circuits using low-intensity, low-frequency ultrasound. PLoS One 2008;3:e3511. https://doi.org/10.1371/journal.pone.0003511.